



Contents lists available at ScienceDirect

Journal of King Saud University – Science

journal homepage: [www.sciencedirect.com](http://www.sciencedirect.com)

Original article

# Aseismic and seismic impact on development of soft-sediment deformation structures in deep-marine sand-shaly Crocker fan in Sabah, NW Borneo

Muhammad Jamil<sup>a,b,\*</sup>, Numair Ahmed Siddiqui<sup>a,c,\*</sup>, Muhammad Umar<sup>d</sup>, Muhammad Usman<sup>e</sup>, Nisar Ahmed<sup>a</sup>, Abdul Hadi Abd Rahman<sup>a</sup>, Faisal Kamal Zaidi<sup>f</sup><sup>a</sup> Department of Geosciences, Universiti Teknologi PETRONAS, Seri Iskandar, 32610 Perak, Malaysia<sup>b</sup> Department of Earth Sciences, COMSATS University Islamabad, Abbottabad Campus, 22044 KPK, Pakistan<sup>c</sup> Shale Gas Research Group, Institute of Hydrocarbon Recovery, Universiti Teknologi PETRONAS, Seri Iskandar, 32610 Perak, Malaysia<sup>d</sup> Department of Earth Sciences, The University of Haripur, 22620 KPK, Pakistan<sup>e</sup> Department of Earth and Environmental Sciences, University of Milano-Bicocca, Piazza Della Scienza 4, 20126 Milano, Italy<sup>f</sup> Department of Geology, College of Science, King Saud University, 11451 Riyadh, Saudi Arabia

## ARTICLE INFO

### Article history:

Received 4 February 2021

Revised 25 April 2021

Accepted 12 June 2021

Available online 19 June 2021

### Keywords:

Soft-sediment deformation structures (SSDSs)

Deep-marine sand-shaly fan

Seismites

West Crocker Formation

Sabah Basin

NW Borneo

## ABSTRACT

Soft-sediment deformation structures are present within the deep-marine fan of the West Crocker Formation, Sabah Basin, NW Borneo. Focus of this study is to highlight the impact of seismic and aseismic activities on the development of these structures and their distribution in deep-marine fan. Twenty-nine types of deformation structures were identified during the study of twelve exposed sections. These structures were grouped into five categories: i) water-escape structures, ii) sole marks, iii) clastic intrusions, iv) deformed laminations, and v) syn-depositional brittle and ductile deformation structures. The sediment deformation is interpreted to be caused either by aseismic processes like slope failure, gravity collapse, sediment overloading, density gradient, seismic induced mechanisms such as earthquakes, tectonic uplift, or combined effect of seismic and aseismic events. These structures are classified based on type of features developed during semi-consolidated phase of rock deposition. The seismites structures i.e., clastic intrusions, deformed laminations, and syn-depositional structures are correlated with active collisional tectonics during the Late Paleogene times in the Sabah Basin. In the present work, a generalized conceptual model has also been proposed for the development of soft-sediment deformation structures in a sub-marine fan environment. Dewatering structures and rapid sedimentation features are associated with inner fan, load and flame structures are present within middle fan, while contorted layers, slumps and mass-transport deposits are linked with distal fan settings.

© 2021 The Author(s). Published by Elsevier B.V. on behalf of King Saud University. This is an open access article under the CC BY license (<http://creativecommons.org/licenses/by/4.0/>).

## 1. Introduction

Genetic mechanisms and morphological characterization of sedimentary structures are vital for understanding of geological history and depositional processes active in a sedimentary basin (Liu et al.,

2016; Gao et al., 2020). In siliciclastic rocks, soft-sediment deformation structures (SSDSs) are developed during or earlier phase of rock deposition, mostly in semi-consolidated phase of sediments prior to diagenesis. This deformation is also termed as penecontemporaneous or pre-lithification deformation (Owen et al., 2011). Fluidization and liquefaction phenomena contribute significantly to the development of SSDSs. However, a clear understanding, exact origin, and timing of development of sediment deformation structures are still ambiguous (Al-Mufti and Arnott, 2020).

Various geological events like tsunamis, storm waves, and earthquakes (Moretti and Sabato, 2007) are responsible for the development of SSDSs. The factors that determine the development of soft-sedimentary structures are consolidation, saturation level, type of lithology, depth of sediment accumulation, intensity and epicenter of earthquakes (Liu et al., 2016). These SSDSs are also termed as

\* Corresponding authors at: Department of Geosciences, Universiti Teknologi PETRONAS, Seri Iskandar, 32610 Perak, Malaysia.

E-mail addresses: [jamil287@gmail.com](mailto:jamil287@gmail.com) (M. Jamil), [numair.siddiqui@utp.edu.my](mailto:numair.siddiqui@utp.edu.my) (N.A. Siddiqui).

Peer review under responsibility of King Saud University.



Production and hosting by Elsevier

seismites when triggered by the seismic activity (Singh and Jain, 2007). By using the deep-marine Crocker Formation of Sabah Basin as a case study (Fig. 1a,b), this research aims to characterize the occurrence of SSDSs, their spatial distribution in various architectural elements of a submarine fan, and relationship of seismites with collisional tectonic regime of the Sabah Basin during the Late Paleogene times.

## 2. Geological background

Deep-marine sediments of the Late Paleogene age are extensively outcropped in the West Sabah which are generally termed as Crocker sands because of dominant sandstone lithology (Jackson et al., 2009; Zakaria et al., 2013; Sheikh et al., 2021). The younger sediments are termed as Late Paleogene Crocker sediments to differentiate them from Early Paleogene Rajang Group (comprising of Trusmadi and East Crocker formations (Fig. 1c) (Abdullah et al., 2017). Hence, the term West Crocker Formation is now restricted

to only those Late Paleogene sediments which are bounded by unconformable stratigraphic surfaces (Jamil et al., 2019, 2020).

Regionally, Borneo has a complex history of sedimentation and tectonics that resulted in the development of massive accumulation of deep-marine sediments during the Early Cenozoic era. (Mathew et al., 2014; Siddiqui et al., 2019; Usman et al., 2020; Ahmed et al., 2021a, 2021b). Sabah Basin is located in northern part of the Borneo that lies at complex junction of the South China Sea in the West, Celeb Sea in the SE, and Sulu Sea in the NE (Siddiqui et al., 2017, 2020; Usman et al., 2021). Previously, few sedimentary structures like flute marks, cross-bedding, convolution, parallel laminations, sand injectites and dish structures had been reported in this formation (Jackson et al., 2009; Zakaria et al., 2013; Madon, 2020; Jamil et al., 2021).

## 3. Data and methods

The geological field locations are mainly affected by compressional tectonic regime which is evident from vertically oriented

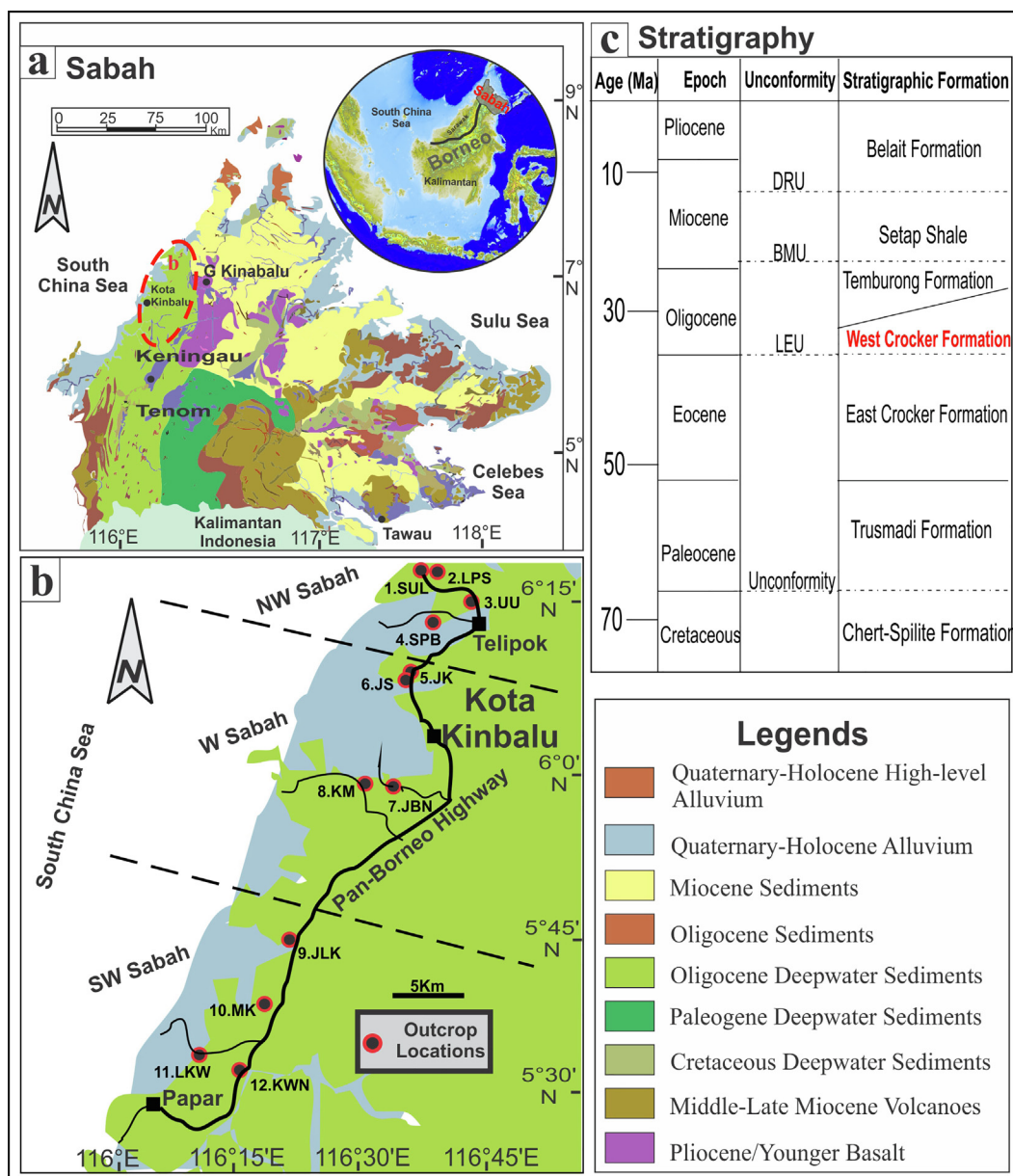


Fig. 1. Location of study area. a) regional map of NW Borneo with encircled Sabah area. b) location of twelve outcrops 1 to 4 in NW Sabah, locations 5–8 in West Sabah and 9–12 in SW Sabah. c) stratigraphy of the West Sabah.

stratigraphic sections. The transect selected for detailed sedimentary logging with deformation structures extends from NW Sabah (location 1: Jalan Sulaman near Telipok) to SW Sabah (location 12: Kawang) which is about 47.6 km in length along the Pan-Borneo Highway, Sabah (Fig. 2). Cumulative vertical thickness of all field logs for these exposed sections is about 877.40 m. Generally, this stratigraphic formation was deposited in deep-marine environment therefore most of the sandstone beds are structureless and do not bear any deformation structures. However, SSDSs were marked, located, and identified at several stratigraphic intervals in the geological field (Fig. 2). These sedimentary features were later interpreted in the light of previous literature to determine the geological processes active during the deposition in the respective sedimentary basin.

#### 4. Results and interpretation

Twenty-nine types of SSDSs were identified which were broadly categorized into five major seismic and aseismic deformation structures in a deep-marine environment (Table 1). The sedimentary structures discussed in this study were identified at several stratigraphic levels within the West Crocker Formation. These features are classified based on geological processes responsible for the development of deformation structures including dewatering, overloading, intrusion, syn-depositional brittle, and ductile deformation structures.

##### 4.1. Water-escape structures

###### 4.1.1. Dish structures

Small saucers (dishes), which are sometimes separated by vertical columns, represent the escape of pore-water in an upward direction during lithification of sediments. The size of dishes vary from 1 to 3 cm and morphology is mainly concave up structures

in an undulated linear fashion. These structures are rare in NW and SW Sabah, but they are abundant in the West Sabah. The sandstone units in the West Sabah are relatively clean therefore, these structures are faint. Generally, the dewatering structures are common in thick to massive muddy sandstones (Fig. 3a). Few examples of dish structures have also been identified at Jalan UMS behind KFC (JK) section, West Sabah (Fig. 3b), which are interpreted to be deformed by earthquakes (Zeng et al., 2018).

###### 4.1.2. Water-escape cusp

Cusp mainly occur in between two coarsening up sandstone units when the sediments are still in phase of fluidization (Owen, 1996). They are columnar generally vertical and similar in shape like the flame structure (Ali and Ahmad Ali, 2018). The zone of cusp structures ranges from 4 to 7 cm and width from 1 to 11 cm (Fig. 3c). These cusp structures are relatively less common as compared to traditional dish structures in the study area. In general, the seismic impact or abrupt overpressure resulted in the movement of water from unlithified sediments and consequently develops water-escape structures (Owen, 1996).

##### 4.2. Sole marks

###### 4.2.1. Flame structures

Flame structures are usually developed in shaly unit overlying sandstone, or in muddy sandstone overlying clean sandstone unit. The mud flames are equally developed in shale laminae (Fig. 3d) bounded by sandstone intervals. However, the morphology of flame is like mud injection in rare cases (Fig. 3e), axe-shaped (Fig. 3f) or linear wedge structure (Fig. 3g). Sometimes the flame structure is less developed due to very thin mud lamina and is termed as slight flame expression (Fig. 3h). The flame dimensions vary in size from less than 1 cm (Fig. 3h) to more 5 cm in flame height (Fig. 3g). The triggering process for development of flame

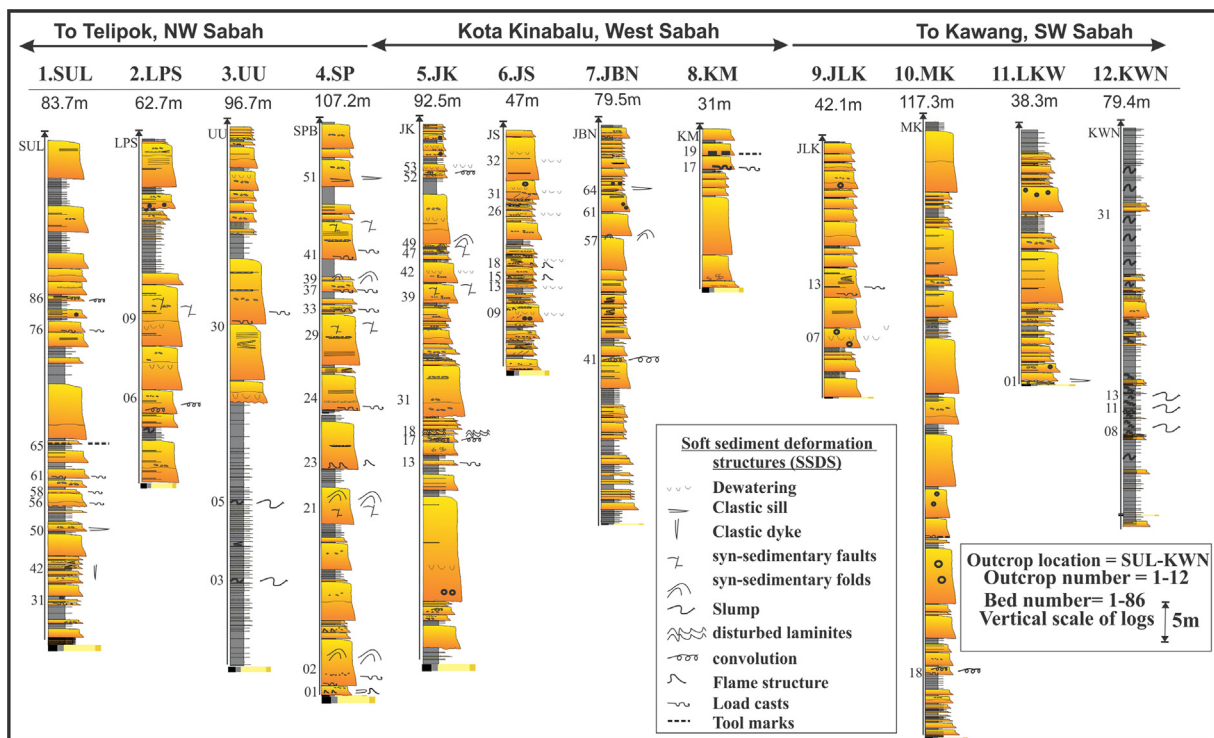


Fig. 2. Distribution of SSDSs in twelve exposed sections, four from NW Sabah (1.SUL Jalan Sulaman section, 2.LPS Lapanan road section 3.UU University Utama section 4.SP Sepanggar road section), four locations around Kota Kinabalu (5.JS Jalan UMS road section, 6.JK Jalan UMS behind KFC section, 7.JBN Jalan Bantayan section, 8.KM Kampung Madpai section), and four sections in SW Sabah (9.JLK Jalan Lok Kawi section, 10.MK Kampung Mook section, 11.LKW Lok Kawi wildlife road section 12.KWN Kawang section).

**Table 1**  
Summary of twenty-nine types of SSDSs with five major types of groups interpreted with respect to deformation processes and triggering mechanisms.

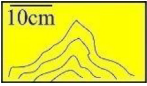


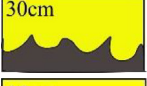
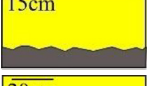

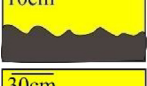

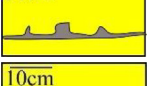
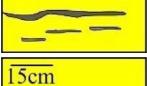
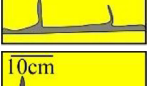
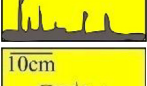

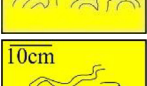
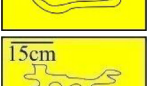


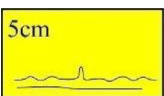

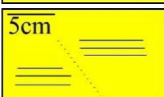
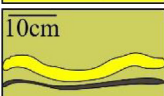
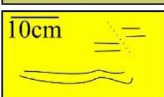



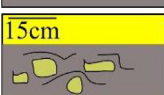
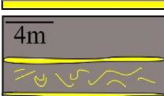
No.	Types of SSDSs	Description	Type of groups	Figure	Processes	Mechanisms
1		Dish structures	Dewatering structures	3a, 3b	abrupt overpressure	Seismic or rapid sedimentation
2		Water-escape cusp		3c	flow pathways in fluidized sediments	Influence of pore pressure
3		Developed mud flames	Sole marks and flame structures	3d-3g	shale penetrates sand base	Reverse density gradient or seismic shock
4		Slight flame structure		3h	density contrast allows mud to move upward	Compensate sand pressure on mud
5		Load casts		4a	uneven loading	Gravitational instabilities, seismic origin
6		Pseudonodule		4b	heavier material sinks into mud	Sediment loading
7		Flute casts		4c	density loading	Erosional currents
8		Tool marks		4d	sagging, sand over mud drag	Density gradient
9		Detach sandnodule		4e	uneven loading	Dense sand nodules sink into mud
10		Ball and pillow		4f	disturbed sand base moves down into mud	Reverse density gradient, seismic activity
11		Sill ± faults	Clastic intrusions	5a-c, 5e	intrusion and displacement	Seismic or tectonics
12		Mud sill with dyke		5d	intrusion with variable stress directions	Co-seismic liquefaction
13		Minor mud dykes		5f	upward bedding of mud layer	Co-seismic liquefaction
14		Large mud dykes		5g	vertical injections	Seismic activity
15		Overturned convolution	Defromed laminations	6a	deformed laminae with broad hinge	Overloading or rapid sedimentation
16		Multiple convolution		6b, 6c	amalgamated sand overlain small structures	Differential liquefaction
17		Chaotic convolution		6d	convolution associated with silt unit	Gravitational movement
18		Convolution with mud		6e	crumpling of silty laminations	Differential liquefaction
19		Multiple laminites		6f	lamiantions are slightly bended	Ductile laminae deformation



Table 1 (continued)

No.	Types of SSDSs	Description	Type of groups	Figure	Processes	Mechanisms
20		Disturbed laminites		6g	small-scale overloading	Injection with slight bending
21		Multiple syn-sedimentary faults	Syn-depositional structural deformation	7a, 7b	array of faults due to continuous stress	Tectonic or seismic shocks
22		Syn-sedimentary fault		7c, 7d	localized stress	Seismic event or other short-lived mechanism
23		Syn-sedimentary fold		7e	ductile deformation phase	Compressional phenomenon
24		Syn-sedimentary fault and fold		7f, 7g	brittle and ductile deformation	Differential stress behaviour
25		Syn-sedimentary Fault propagation fold		7h	initially folding and later faulting	Convergent tectonic mechanism
26		Contorted layers		8a, 8d	individual lamina differentially deform	Seismic episodes
27		Chaotic slumping		8b, 8c	deformed Silty mud incorporate into sand	Minor chaotic event
28		Slump with sand clasts		8e, 8f	rotational component in chaos	Gravitational collapse
29		Mass-transport complex		8g, 8h	complex orientation of lithology	Slope failure, gravitational collapse

include gravity loading (Ge and Zhong, 2018), or seismic shear (Zeng et al., 2018).

#### 4.2.2. Load structures

Deep-marine deposits with alternate sand-shale lithology (competence contrast) are often characterized by load structures. The range of deformation varies significantly where lateral continuity of these load structures is limited, and they are developed in form of symmetrical spheres as well as asymmetrical geometries (Fig. 4a, 4b). Brief expressions of flute casts (Fig. 4c) and tool marks (Fig. 4d) are present in the West Sabah interpreting the deformation associated with drag movement of sediments during the high-density cohesive gravity flow (Peakall et al., 2020).

#### 4.2.3. Pseudonodules

Variable shapes and morphologies of detached and isolated nodules are entrenched in an underlying lithology (Fig. 4e) having density contrast are termed as pseudonodules (Ali and Ahmad Ali, 2018). The diameter of irregular spheroidal morphologies varies from 3 to 9 cm while the long axes vary from 8 to 14 cm and short axes from 4 to 9 cm. These pseudonodules are interpreted to be the result of sediment loading of more dense sand in underlying shale interval (Rodríguez-Pascua et al., 2000).

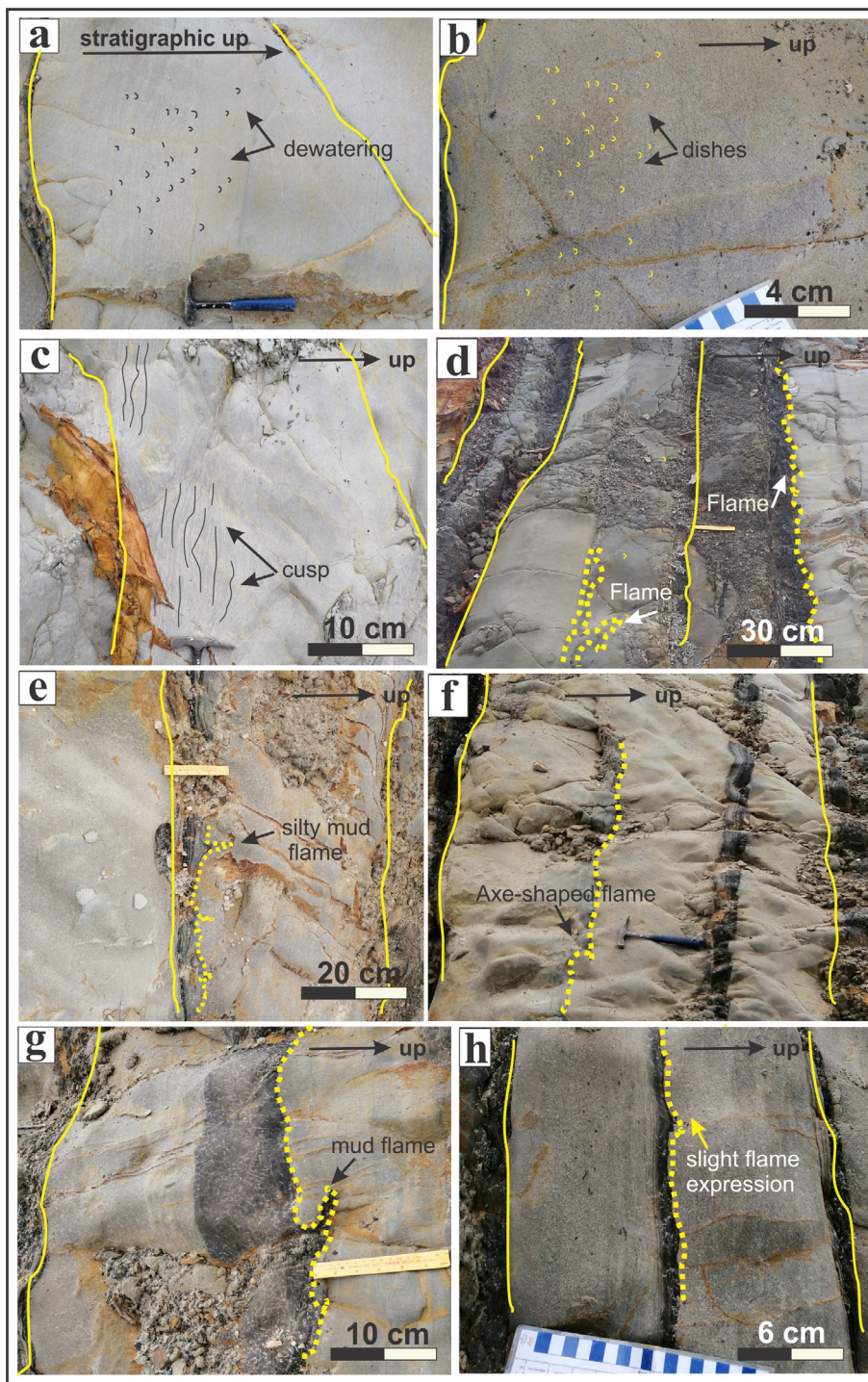
#### 4.2.4. Ball and pillow structures

The sandstone layer is divided into many concentric pillows which are nearly spherical or ellipsoidal. These individual plano-convex pillow shapes can either be isolated masses or partially connected (McLaughlin and Brett, 2004). The diameter of pillows varies from 8 to 23 cm, while the ball diameter ranges only from 4 to 11 cm (Fig. 4f). Ball and pillow structures are formed by reverse density gradient as well as seismic impact on semi-consolidated sediments (Obermeier, 1996).

### 4.3. Soft-sediment intrusions

#### 4.3.1. Clastic sills

Bedding parallel mud intrusions are present in various forms where the width of mud sill is less than 1 cm, but the length is more than 40 cm (Fig. 5a, b). Clastic sills are associated with syn-depositional faulting (Fig. 5c) are less common in depositional record. These mud sills are rarely associated with mud dykes (dyke off-shoots from the parent sill structure) as in the Jalan Bantayan site, West Sabah (Fig. 5d). In some cases, clean sand sill is intruded into the muddy sand unit (Fig. 5e). Due to limited lateral continuity, these clastic sills are interpreted to be developed by seismic triggering mechanism (Madon, 2020).



**Fig. 3.** Dewatering and flame structures a) dewatering columns in massive sandstone. b) dish structures in sandstone with mud laminae. c) water-escape cusp in massive sandstone. d) developed flame structure at the base of overlying sand beds. e) silty mud flame developed in between sand bed. f) axe-shaped flame structure bounded by two sandstone intervals. g) wedge-shaped flame structure developed by underlying mud unit. h) slight effect of flame by thin mud unit into overlying sand bed.

#### 4.3.2. Clastic dykes

Sand or mud filled linear features, that cut across the adjacent layers vertically or at an angle, have size from centimeters to meter scale (Kumar et al., 2020). In the studied sections, clastic dykes are mainly intruded vertically into older strata with length of about 2–5 cm (Fig. 5f). These mud dykes are often injected vertically into medium to thick bedded sandstone unit with variable width from 0.8 cm to 2.3 cm at multiple points and length of dykes may exceeds 20 cm (Fig. 5g). The existence of dykes in the studied area

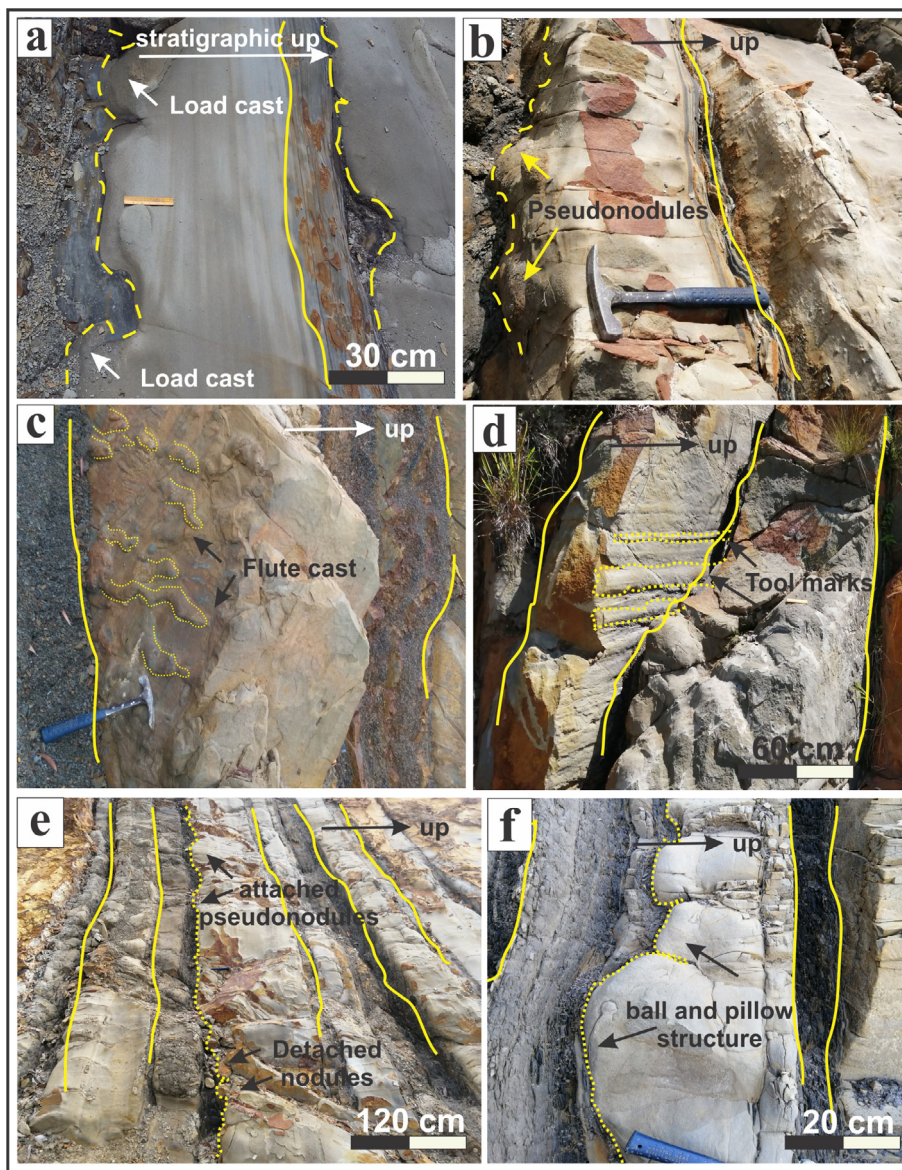
indicate the impact of paleo-seismic activity in form of moderate to high magnitude earthquakes (Rodríguez-Pascua et al., 2000).

#### 4.4. Deformed lamination structures

##### 4.4.1. Convolute laminations

Complex folding and crumpling of laminations in a sedimentary unit is termed as convolution (Kumar et al., 2020). Overturned convolute laminations are present with broad hinge area in Jalan





**Fig. 4.** Sole marks and load structures. a) load casts at the base of sandstone unit. b) Pseudonodules developed due to sediment loading. c) flute casts representing the effect of erosional currents. d) tool marks at the base of sandstone. e) undulating sandstone base and detached nodules due to sinking of dense sandstone into underlying shale unit. f) ball and pillow structure formed at base of sandstone.

Sulaman section, NW Sabah (Fig. 6a), while multiple convolutions are overlain by structureless massive sandstone unit in the Lapasan section, NW Sabah (Fig. 6b), and Jalan UMS roadside, West Sabah (Fig. 6c). In some cases, these convolute structures may develop a chaotic morphology in clean sandstone (Fig. 6d) as well as in form of silty mud laminations (Fig. 6e). The convolutions extend in length from 28 to 67 cm along the strike of bed and range in width from 6 to 21 cm. However, the intensity of deformation or folding varies significantly and depending on liquefaction (Koç-Taşgın and Altun, 2019).

4.4.2. Disturbed laminites

Disturbed laminites are often developed in silty sand units contain small-scale deformation which are expressed in multiple morphologies (Fig. 6f). The rock units containing these small-scale structures are massive sandstone having floating mudclasts (Fig. 6f) or sandstone gradually altered into disturbed laminations with mud cap (Fig. 6g). Furthermore, the scale of these structures ranges from 7 mm to 4 cm, interpreted as ductile deformation (Ali and Ahmad Ali, 2018).

4.5. Syn-depositional structural deformation

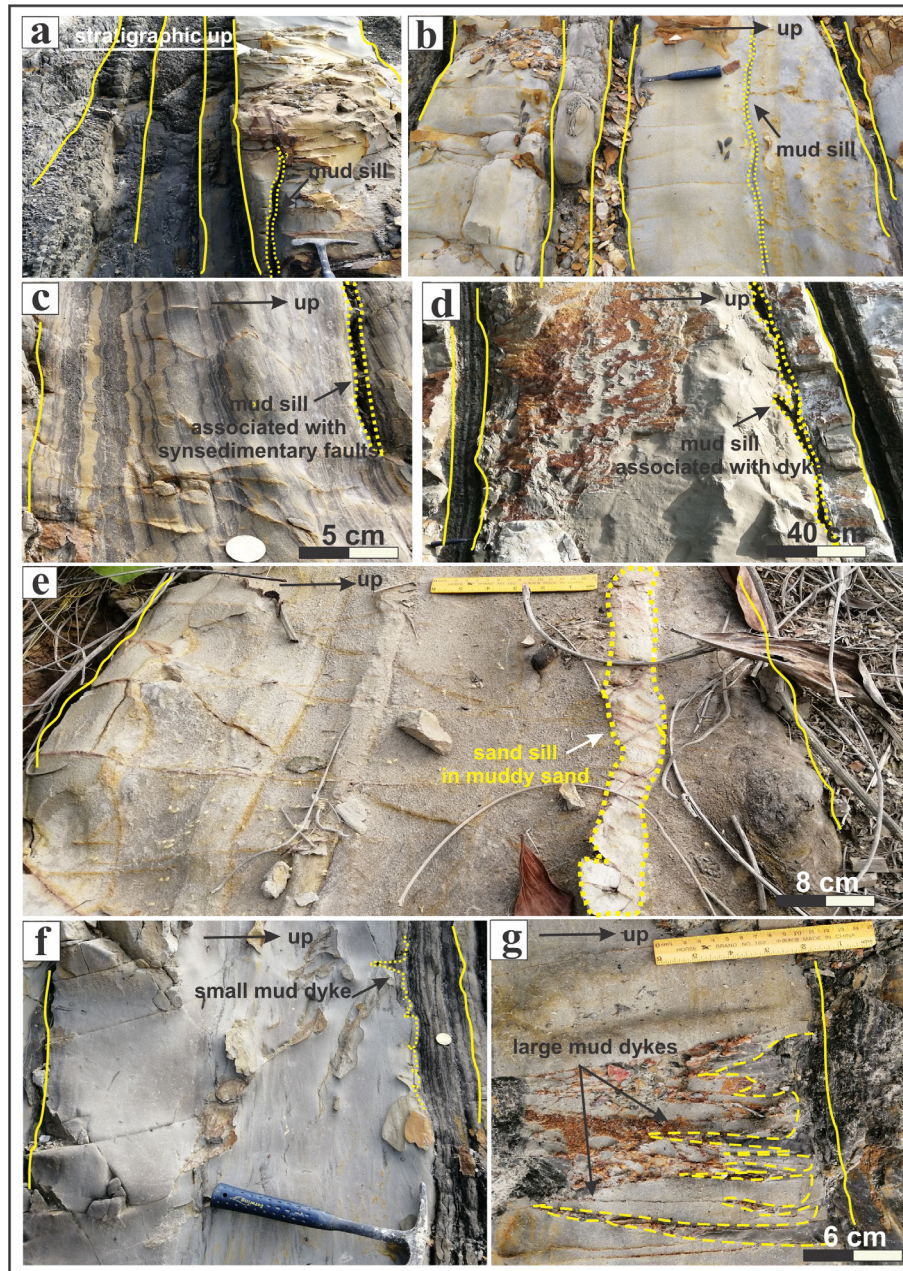
4.5.1. Syn-sedimentary faults

Brittle deformation structures like syn-sedimentary faults are common in heterolithic lithologies in the study area where displacement along the fault plane is normally less than cm scale and bounded by undeformed beds indicating syn-sedimentary origin (Fig. 7a). Most of these faults display reverse dip-slip movement that is associated with compressional stress (Fig. 7b). They are correlated with the subduction and collisional regime of the study area. However, normal syn-sedimentary faults are sporadically present in the studied sections (Fig. 7c,d) indicating a local extensional event (Ko et al., 2017).

4.5.2. Syn-sedimentary folds

Syn-sedimentary folds having broad or narrow area of fold axis (Fig. 7e-g) are present in the Sepanggar section, NW Sabah. These syn-sedimentary folds may also be associated with faults (Fig. 7h) as fault propagation folds. In contrast to syn-sedimentary faults,





**Fig. 5.** Injection or intrusion structures. a) discontinuing mud sill penetrated sandstone unit. b) mud sill into thick sandstone interval. c) mud sill intruded into syn-depositional faulted sandstone. d) sill associated dyke structure in sandstone unit. e) clean sand sill injected into muddy sandstone. f) small mud dykes injected into underlying sandstone interval. g) large mud dykes intruded in sandstone at multiple points.

most of the syn-depositional folds are related to clean sandstone units (Fig. 7e), while few syn-sedimentary folds are linked with heterolithic beds (Fig. 7h). The underlying and overlying units are both undeformed that indicate seismic events responsible for these deformation structures (Marco and Agnon, 2005).

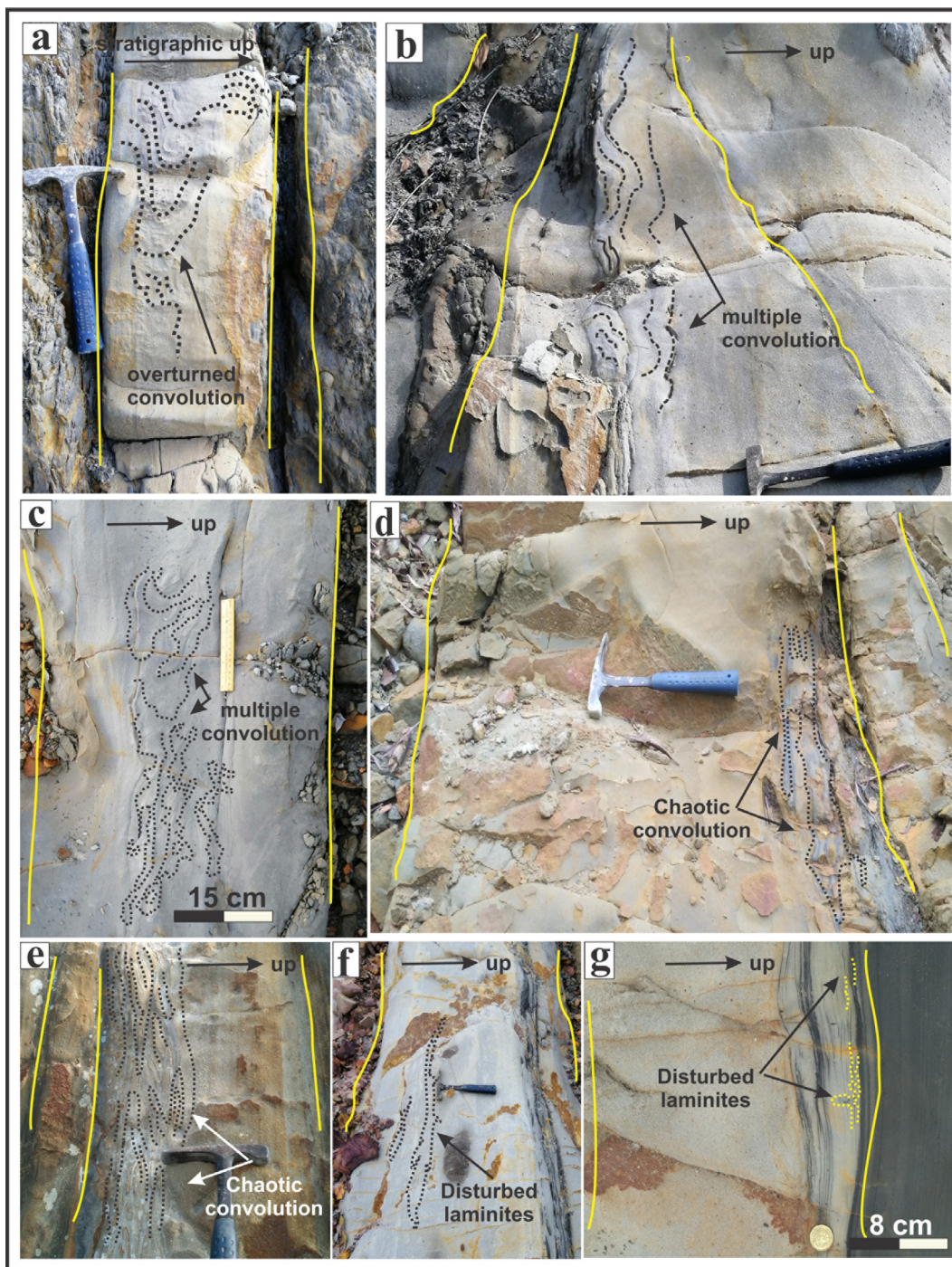
#### 4.5.3. Slump structures and mass-transport deposits

Slump units are present in silty shale (Fig. 8a), in sandstone with silty lumps (Fig. 8b), and/or patches of muddy sandstone showing chaotic nature with some rotational activity and floating mudclasts (Fig. 8c). These minor slump units, with limited lateral continuity, are also termed as contorted layers having multiple small events of slumping (Fig. 8d). The small broken mud and sand

fragments are common in slump beds bounded either by stratified bedding (Fig. 8e) with undulations or rough arrangement of sediments (Fig. 8f). The size of slump may vary from multi-meter (Fig. 8a) to cm level (Fig. 8d) depending on the unit in which slumping took place during the phase of sediment consolidation.

However, presence of various unarranged and partially folded silty shale units (Fig. 8g) in the Kawang section in SW Sabah (Jamil et al., 2020) are interpreted as mass-transport deposits (Fig. 8h) as a result of gravity collapse (Alsop et al., 2019). Furthermore, the presence of repetitive horizons of contorted layers at various levels interpreted to be the result of aseismic trigger; i.e., slope failure (Owen et al., 2011).





**Fig. 6.** Convolutions and disturbed laminites. a) overturned convolution. b) and c) multiple convolutions. d) and e) chaotic convolutions. f) multiple disturbed laminites associated with mudclasts. g) small-scale disturbed laminites overlain by mud cap.

## 5. Discussion

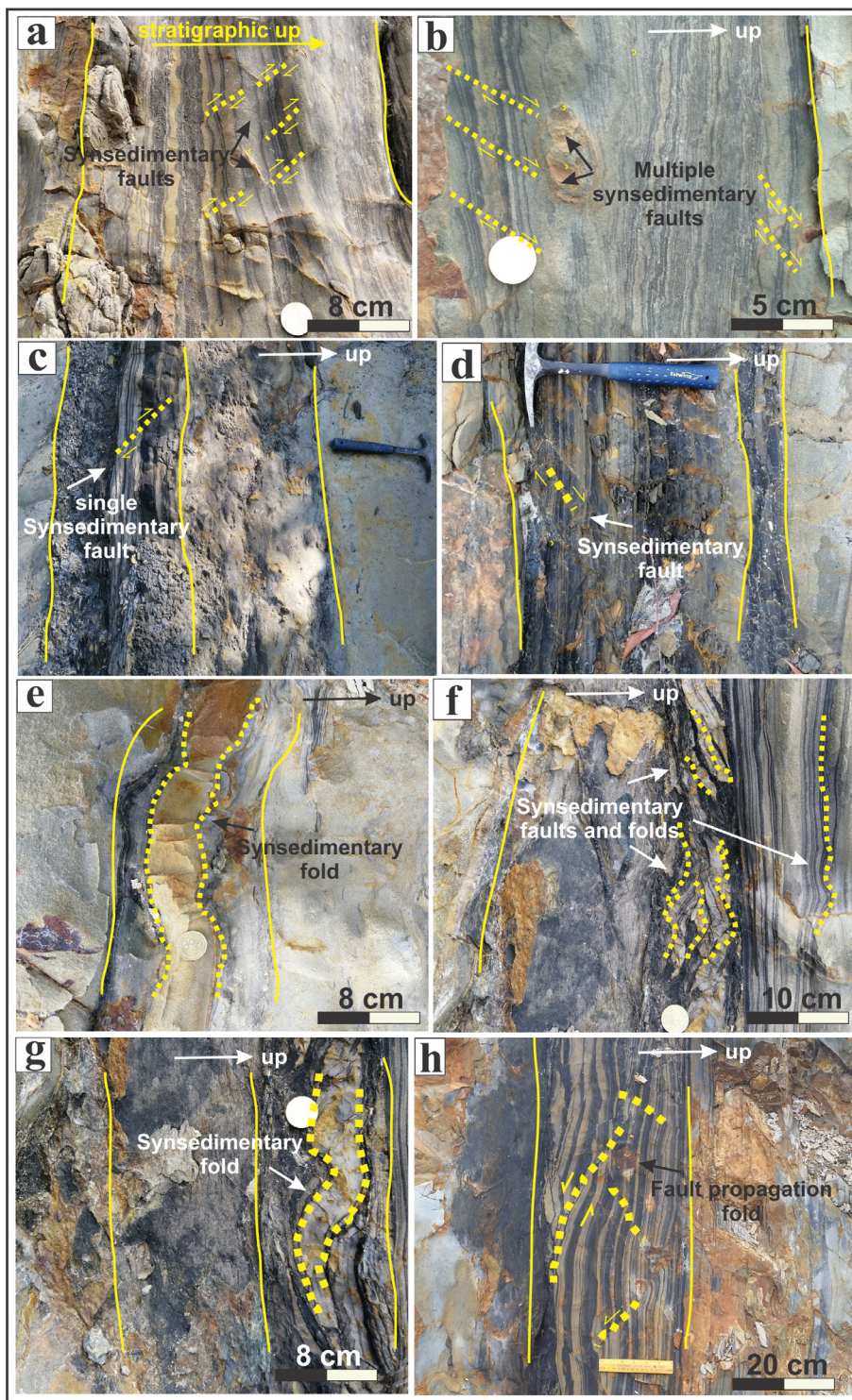
### 5.1. Seismic and aseismic impact

The Sabah Basin was tectonically active in the Late Paleogene times when subduction and collision of South China Sea was active beneath NW Borneo (Hennig-Breitfeld et al., 2019). The existence of sand dykes, mud flames, ball and pillow structures, and syn-sedimentary faults suggest moderate to high magnitude paleo-seismic activity in the area that was responsible for soft-

sediment deformation. However, contorted layers and mass-transport deposits in NW Sabah indicate aseismic origin for the development of SSDs (Alsop et al., 2019). Moreover, convolute laminations are often associated with thick to massive sandstone indicating the rapid sedimentation as a possible aseismic triggering mechanism (Koç-Taşgın and Altun, 2019). The small broken sand blocks in slump suggests the element of slide associated with slump structure due to liquefaction aseismic phenomenon.

However, slump structures could also slightly fold the silty sandstone thin beds and laminae which are not linked with slide





**Fig. 7.** Syn-depositional deformations. a) and b) multiple arrays of *syn*-sedimentary faults. c) and d) localized stress resulted into single *syn*-sedimentary fault. e) slight bending of thin sandstone. f) *syn*-depositional fault and folds overlain by undeformed laminations. g) *syn*-sedimentary folding in sandstone interval. h) fault propagation fold representing a combined effect of brittle and ductile deformations.

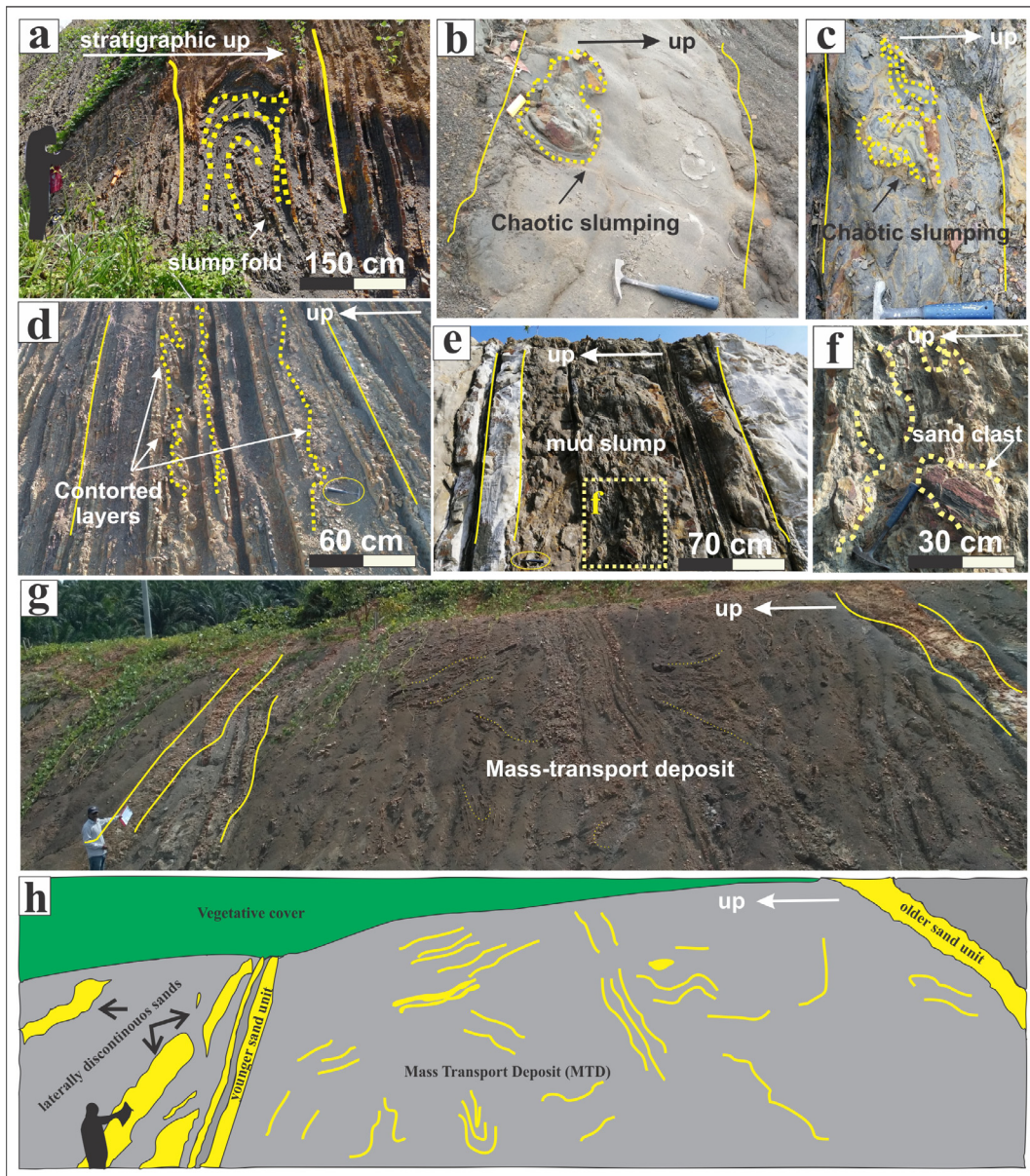
event. They are potentially linked with seismic shocks in unconsolidated sediments (Singh and Jain, 2007). Furthermore, presence of *syn*-sedimentary faults in the Sepanggar, NW Sabah because of localized forces also point out the seismic activity as a possible triggering mechanism (Tongkul, 2017). These sediments having preserved seismic record in form of deformation are termed as seismites that are quite common in active tectonic margins. Large-scale slump structure in deep-marine sediments (NW Sabah)

are interpreted to be the result of earthquake of large magnitude (Bowman et al., 2004).

5.2. Distribution in deep-marine fan

The present study integrates the development and distribution of SSDSs with previously proposed generalized submarine fan models (Fig. 9). The previous literature elaborates the distribution





**Fig. 8.** Syn-depositional structural deformation. a) slump fold. b) and c) chaotic slumping. d) contorted layers. e) and f) sand clasts in mud slump. g) and h) mass-transport deposits in silty shale units.

of SSDs in glacio-lacustrine settings (Pisarska-Jamroży and Woźniak, 2019). However, no such attempt has been made to correlate the occurrence of SSDs and their distribution in deep-marine fan. Initially, facies and facies associations were interpreted for the studied sections and the individual deep-marine architectural elements were identified for entire Crocker submarine fan (Fig. 2). Later, various types of SSDs were interpreted by their distribution a generalized submarine fan settings (DeVay et al., 2000). The gravitational collapse and chaotic structures found to be associated with slopes with broken sand clasts in siliclastic rock successions. Rapid sedimentary influx resulted in massive sand units having floating mudclasts, convection, and dewatering structures associated with proximal fan settings. Alternate medium to thin bedded sand-mud units with load structures are found to be associated with middle fan environment. Minor slump folds and contorted layers are mainly present in silty-shale intervals of outer fan deposits.

## 6. Conclusion

The impact of numerous seismic and aseismic events resulted in the development of wide variety of SSDs including water-escape structures, ball and pillow structures, pseudonodules, load structures, flame structures, intrusion structures and distorted laminations, and *syn*-depositional structures in a submarine fan. Load and flame structures were associated with upper denser interval above lighter lithology and caused deformation due to liquidization of unstable sediments. Uneven loading or density contrasts were linked with instabilities of gravity, whereas ascending evicton of pore fluids attributed to water-escape structures. Convection and *syn*-sedimentary folds were associated with ductile deformation during downslope gravitation movement, while brittle actions contributed the development of *syn*-depositional faults. Gravity and seismic activity were major factors which develop the SSDs in a sedimentary basin. Episodic appearance of *syn*-depositional folds

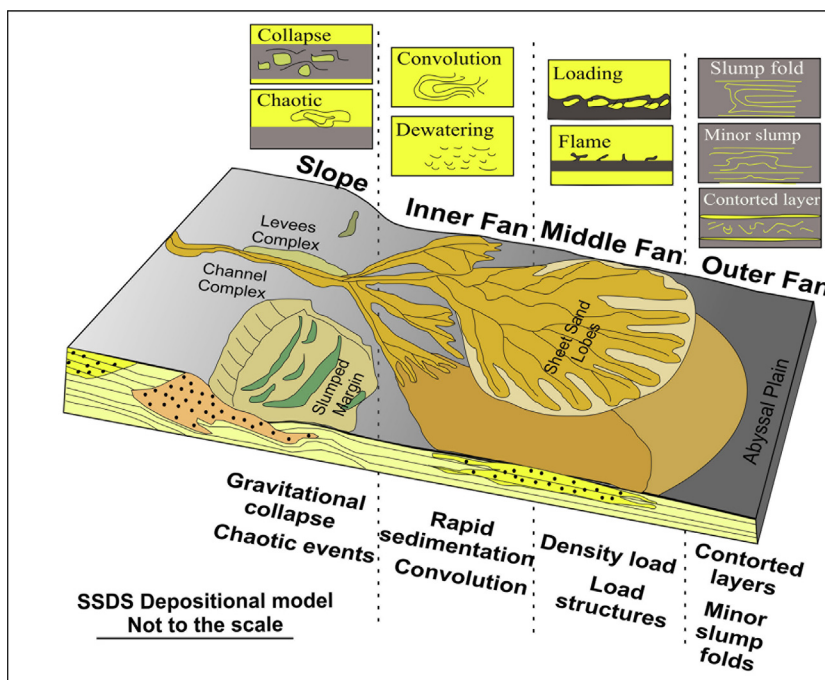


Fig. 9. A conceptual depositional model proposed for the correlation of deep-marine fan with development of SSDS.

and faults in stratigraphic intervals interpreted as seismites which are developed due to seismic events in active tectonic settings. Conclusively, these structures were developed in response to both seismic and aseismic processes that were active at discrete stratigraphic intervals in a deep-marine sedimentary basin. A generalized conceptual model is proposed in this study from inner to outer fan environment; where rapid sedimentation and convolution structures are present in inner fan, load structures in middle fan, and minor slump or contorted layers are confined to outer fan environment.

### Funding

This project was supported by the Petroleum Research Fund (PRF Cost No. 0153AB-A33) awarded to Dr. Eswaran Padmanabhan and Fundamental Research Grant, Ministry of Higher Education (MoHE) Malaysia (Project ID 16880, Reference Code FRGS/1/2019/STG09/UTP/03/1).

### Declaration of Competing Interest

The authors declare that they have no known competing financial interests or personal relationships that could have appeared to influence the work reported in this paper.

### Acknowledgements

The authors express sincere thanks to Shale Gas Research Group (SGRG) and Department of Geosciences, Univeristi Teknologi PETRONAS (UTP) Malaysia for fieldwork and data analysis. The comments and feedback from the reviewers greatly improved the manuscript.

### References

Abdullah, W.H., Togunwa, O.S., Makeen, Y.M., Hakimi, M.H., Mustapha, K.A., Baharuddin, M.H., Sia, S.-G., Tongkul, F., 2017. Hydrocarbon source potential

- of Eocene-Miocene sequence of Western Sabah, Malaysia. *Mar. Pet. Geol.* 83, 345–361.
- Ahmed, N., Siddiqui, N.A., H. B. A. Rahman, A., Jamil, M., Usman, M., Sajid, Z., Kamal Zaidi, F., 2021a. Evaluation of hydrocarbon source rock potential: Deep marine shales of Belaga Formation of Late Cretaceous-Late Eocene, Sarawak, Malaysia. *Journal of King Saud University - Science* 33 (1), 101268. <https://doi.org/10.1016/j.jksus.2020.101268>.
- Ahmed, N., Siddiqui, N.A., Ramasamy, N., Ramkumar, M., Jamil, M., Usman, M., Sajid, Z., Rahman, A.H.B.A., 2021b. Geochemistry of Eocene Bawang Member turbidites of the Belaga Formation, Borneo: Implications for provenance, palaeoweathering, and tectonic setting. *Geological Journal* 56 (5), 2477–2499. <https://doi.org/10.1002/gj.v56.510.1002/gj.4062>.
- Al-Mufti, O.N., Arnott, R.W.C., 2020. The origin and significance of convolute lamination and pseudonodules in an ancient deep-marine turbidite system: From deposition to diagenesis. *J. Sediment. Res.* 90, 480–493.
- Ali, U., Ahmad Ali, S., 2018. Seismically induced soft-sediment deformation structures in an active seismogenic setting: The Plio-Pleistocene Karewa deposits, Kashmir Basin (NW Himalaya). *J. Struct. Geol.* 115, 28–46.
- Alsop, G.I., Weinberger, R., Marco, S., Levi, T., 2019. Identifying soft-sediment deformation in rocks. *J. Struct. Geol.* 125, 248–255.
- Bowman, D., Korjenkov, A., Porat, N., 2004. Late-Pleistocene seismites from Lake Issyk-Kul, the Tien Shan range, Kyrgyzstan. *Sed. Geol.* 163 (3–4), 211–228.
- DeVay, J.C., Risch, D., Scott, E. and Thomas, C., 2000. A Mississippi-Sourced, Middle Miocene (M4), Fine-Grained Abyssal Plain Fan Complex, Northeastern Gulf of Mexico, AAPG Memoir 72/SEPM Special Publication, pp. 109–118.
- Gao, Y.i., Jiang, Z., Best, J.L., Zhang, J., 2020. Soft-sediment deformation structures as indicators of tectono-volcanic activity during evolution of a lacustrine basin: A case study from the Upper Triassic Ordos Basin, China. *Marine and Petroleum Geology* 115, 104250. <https://doi.org/10.1016/j.marpetgeo.2020.104250>.
- Ge, Y., Zhong, J., Tyrrell, S., 2018. Trigger recognition of Early Cretaceous soft-sediment deformation structures in a deep-water slope-failure system. *Geol. J.* 53 (6), 2633–2648.
- Hennig-Breitfeld, J., Breitfeld, H.T., Hall, R., BouDagher-Fadel, M., Thirlwall, M., 2019. A new upper Paleogene to Neogene stratigraphy for Sarawak and Labuan in northwestern Borneo: Paleogeography of the eastern Sundaland margin. *Earth Sci. Rev.* 190, 1–32.
- Jackson, C.-L., Zakaria, A.A., Johnson, H.D., Tongkul, F., Crevello, P.D., 2009. Sedimentology, stratigraphic occurrence and origin of linked debrites in the West Crocker Formation (Oligo-Miocene), Sabah, NW Borneo. *Mar. Pet. Geol.* 26 (10), 1957–1973.
- Jamil, M., Abd Rahman, A.H., Siddiqui, N.A., Ibrahim, N.A., Ahmed, N., 2020. A contemporary review of sedimentological and stratigraphic framework of the Late Paleogene deep marine sedimentary successions of West Sabah, North-West Borneo. *Bulletin of the Geological Society of Malaysia* 69, 53–65.
- Jamil, M., Rahman, A.H.A., Siddiqui, N.A., Ahmed, N., 2019. Deep marine Paleogene sedimentary sequence of West Sabah: contemporary opinions and ambiguities. *Warta Geologi* 45, 198–200.
- Jamil, M., Siddiqui, N.A., Rahman, A.H.B.A., Ibrahim, N.A., Ismail, M.S.B., Ahmed, N., Usman, M., Gul, Z., Imran, Q.S., 2021. Facies Heterogeneity and Lobe Facies



- Multiscale Analysis of Deep-Marine Sand-Shale Complexity in the West Crocker Formation of Sabah Basin, NW Borneo. *Applied Sciences* 11 (12), 5513. <https://doi.org/10.3390/app11125513>.
- Ko, K., Kim, S.W., Lee, H.-J., Hwang, I.G., Kim, B.C., Kee, W.-S., Kim, Y.-S., Gihm, Y.S., 2017. Soft sediment deformation structures in a lacustrine sedimentary succession induced by volcano-tectonic activities: An example from the Cretaceous Beolgeomri Formation, Wido Volcanics, Korea. *Sed. Geol.* 358, 197–209.
- Koç-Taşgın, C., Altun, F., 2019. Soft-sediment deformation: deep-water slope deposits of a back-arc basin (middle Eocene-Oligocene Kırkgeçit Formation, Elazığ Basin), Eastern Turkey. *Arabian Journal of Geosciences* 12 (24). <https://doi.org/10.1007/s12517-019-4872-4>.
- Kumar, N., Mohan, K., Dumka, R.K., Chopra, S., 2020. Soft Sediment Deformation Structures in Quaternary Sediments from Dadra and Nagar Haveli, Western India. *J. Geol. Soc. India* 95 (5), 455–464.
- Liu, L., Zhong, Y., Chen, H., Xu, C., Wu, K., 2016. Seismically induced soft-sediment deformation structures in the Palaeogene deposits of the Liaodong Bay Depression in the Bohai Bay basin and their spatial stratigraphic distribution. *Sed. Geol.* 342, 78–90.
- Madon, M., 2020. Sand injectites in the West Crocker Formation, Kota Kinabalu, Sabah. *Bulletin of the Geological Society of Malaysia* 69, 11–26.
- Marco, S., Agnon, A., 2005. High-resolution stratigraphy reveals repeated earthquake faulting in the Masada Fault Zone, Dead Sea Transform. *Tectonophysics* 408 (1–4), 101–112.
- Mathew, M.J., Siddiqui, N.A., Menier, D., 2014. An evolutionary model of the near-shore Tinjar and Balingian Provinces, Sarawak, Malaysia. *International Journal of Petroleum and Geoscience Engineering* 2, 81–91.
- McLaughlin, P.I., Brett, C.E., 2004. Eustatic and tectonic control on the distribution of marine seismites: examples from the Upper Ordovician of Kentucky, USA. *Sed. Geol.* 168 (3–4), 165–192.
- Moretti, M., Sabato, L., 2007. Recognition of trigger mechanisms for soft-sediment deformation in the Pleistocene lacustrine deposits of the Sant’Arcangelo Basin (Southern Italy): Seismic shock vs. overloading. *Sed. Geol.* 196 (1–4), 31–45.
- Obermeier, S.F., 1996. Use of liquefaction-induced features for paleoseismic analysis—an overview of how seismic liquefaction features can be distinguished from other features and how their regional distribution and properties of source sediment can be used to infer the location and strength of Holocene paleo-earthquakes. *Eng. Geol.* 44 (1–4), 1–76.
- Owen, G., 1996. Experimental soft-sediment deformation: structures formed by the liquefaction of unconsolidated sands and some ancient examples. *Sedimentology* 43 (2), 279–293.
- Owen, G., Moretti, M., Alfaro, P., 2011. Recognising triggers for soft-sediment deformation: Current understanding and future directions. *Sed. Geol.* 235 (3–4), 133–140.
- Peakall, J., Best, J., Baas, J.H., Hodgson, D.M., Clare, M.A., Talling, P.J., Dorrell, R.M., Lee, D.R., Felletti, F., 2020. An integrated process-based model of flutes and tool marks in deep-water environments: Implications for palaeohydraulics, the Bouma sequence and hybrid event beds. *Sedimentology* 67 (4), 1601–1666.
- Pisarska-Jamrozý, M., Woźniak, P.P., 2019. Debris flow and glacioisostatic-induced soft-sediment deformation structures in a Pleistocene glaciolacustrine fan: The southern Baltic Sea coast, Poland. *Geomorphology* 326, 225–238.
- Rodríguez-Pascua, M.A., Calvo, J.P., De Vicente, G., Gómez-Gras, D., 2000. Soft-sediment deformation structures interpreted as seismites in lacustrine sediments of the Prebetic Zone, SE Spain, and their potential use as indicators of earthquake magnitudes during the Late Miocene. *Sed. Geol.* 135 (1–4), 117–135.
- Sheikh, N.A., Jamil, M., Ling Chuan Ching, D., Khan, I., Usman, M. and Sooppy Nisar, K., 2021. A generalized model for quantitative analysis of sediments loss: A Caputo time fractional model. *J. King Saud Univ. – Sci.* 33, 101179.
- Siddiqui, N.A., Mathew, M.J., Ramkumar, M., Sautter, B., Usman, M., Abdul Rahman, A.H., El-Ghali, M.A.K., Menier, D., Shiqi, Z., Sum, C.W., 2020. Sedimentological characterization, petrophysical properties and reservoir quality assessment of the onshore Sandakan Formation, Borneo. *J. Petrol. Sci. Eng.* 186, 106771. <https://doi.org/10.1016/j.petrol.2019.106771>.
- Siddiqui, N.A., Rahman, A.H.A., Sum, C.W., Mathew, M.J., Hassaan, M., Menier, D., 2017. Generic hierarchy of sandstone facies quality and static connectivity: an example from the Middle-Late Miocene Miri Formation, Sarawak Basin, Borneo. *Arabian Journal of Geosciences* 10, 237.
- Siddiqui, N.A., Ramkumar, M.u., Rahman, A.H.A., Mathew, M.J., Santosh, M., Sum, C. W., Menier, D., 2019. High resolution facies architecture and digital outcrop modeling of the Sandakan formation sandstone reservoir, Borneo: Implications for reservoir characterization and flow simulation. *Geosci. Front.* 10 (3), 957–971.
- Singh, S., Jain, A.K., 2007. Liquefaction and fluidization of lacustrine deposits from Lahaul-Spiti and Ladakh Himalaya: Geological evidences of paleoseismicity along active fault zone. *Sed. Geol.* 196 (1–4), 47–57.
- Tongkul, F., 2017. Active tectonics in Sabah—seismicity and active faults. *Bulletin of the Geological Society of Malaysia* 64, 27–36.
- Usman, M., Siddiqui, N.A., Mathew, M., Zhang, S., El-Ghali, M.A.K., Ramkumar, M.u., Jamil, M., Zhang, Y., 2020. Linking the influence of diagenetic properties and clay texture on reservoir quality in sandstones from NW Borneo. *Mar. Pet. Geol.* 120, 104509. <https://doi.org/10.1016/j.marpetgeo.2020.104509>.
- Usman, M., Siddiqui, N.A., Zhang, S., Mathew, M., Jamil, M., Zhang, Y. and Ahmed, N., 2021. 3D Geo-Cellular Static Virtual Outcrop Model and its Implications for Reservoir Petro-Physical Characteristics and Heterogeneities. *Petroleum Science*, 18, in press.
- Zakaria, A.A., Johnson, H.D., Jackson, C.-L., Tongkul, F., 2013. Sedimentary facies analysis and depositional model of the Palaeogene West Crocker submarine fan system, NW Borneo. *J. Asian Earth Sci.* 76, 283–300.
- Zeng, M., Etensohn, F.R., Spangenberg, J.E., 2018. Bedding-parallel lenticular soft-sediment deformation structures: A type of seimite in extensional settings?. *Tectonophysics* 747–748, 128–145.